Biogeosciences
Open Access
Discussions
EGU

1

2

3

4

5

6

7

Assessment of paleo-ocean pH records from boron isotope ratio in the Pacific

and Atlantic ocean corals: Role of anthropogenic CO_2 forcing and

oceanographic factors to pH variability

11

12

*Mohd Tarique and Waliur Rahaman

National Centre for Polar & Ocean Research, Goa

15

16

17

18
19

20

21

Corresponding: tarique@ncaor.gov.in

23

24

Biogeosciences
Discussions

Abstract

Boron isotopes (δ^{11}B) records from tropical ocean corals have been used to reconstruct paleo-pH of ocean for the past several decades to few centuries which are comparable to the resolution of instrumental records. In most of the studies, attempts have been made to decipher the role of anthropogenic CO_2 forcing to recent trend of ocean acidification based on δ^{11}B derived paleo-pH records. However, such attempts in past were often hindered by limited knowledge of oceanographic factors that contributed to past pH variability and changes. In this study, we have evaluated pH records reconstructed using δ^{11}B records from the Pacific and the Atlantic Oceans corals and investigated major forcing factors that contributed to sub annual-decadal scale pH variability and changes since the industrial era ~1850 AD.

To the best of our knowledge, total eight δ^{11}B records from the Pacific and two from the Atlantic Oceans are available in published literatures. The compilations of these records show large variability; range between 26.27 - 20.82 ‰ which corresponds to pH range 8.40 - 7.63 respectively. Our investigation of pH records from the Pacific ocean based on principal component analysis (PCA) reveals that atmospheric CO_2 can explains maximum up to ~26% of the total pH variability during 1950 – 2004 AD, followed by the ocean-climate oscillations (i.e. ENSO and PDO) driven oceanographic factors up to ~17%. The remaining large variability (~57%) could not be explained by above forcing factors and hence we invoke possible influence of metabolic processes of corals and/or changes in micro-environments within the reefs which are often neglected in interpreting paleo-pH records. Therefore, we highlight the need for detailed investigation in future studies to understand about the exact

48   mechanism, processes/factors that controlled boron isotope fractionations in coral reef

49   environments. Further, our investigation reveals that amplitude of the ENSO driven pH

50   variability shows fivefold increase during 1980 – 2000 AD compared to the previous

51   three decades (1950 – 1980 AD). This observation is consistent with the historical

52   records of global coral bleaching events and therefore underscores role of ENSO

53   driven environmental stress responsible for coral bleaching events. Considering model

54   based projections of increasing frequency and amplitude of extreme ENSO events in

55   the backdrop of recent global warming, bleaching events are likely to increase in the

56   next decades/centuries.

57

58   **Key words**

59   Anthropocene; Boron Isotope; Paleo-pH; Ocean acidification

60   **Key points**

61   • Coral $\delta^{11}B$ records show discernable trend since industrial era ~1850 AD with

62   more rapid declining trend since 1970.

63   • Atmospheric CO_2 together with ocean-climate oscillations driven oceanographic

64   factors can explain maximum upto 43% of the total pH variability in the Pacific.

65   • Atmospheric CO_2 rise contributed to 0.05 unit reduction in pH in the Pacific

66   Ocean during 1950 – 2004 AD.

67   • ENSO driven pH variability increased by fivefold during the last three decades.

68   • Coral bleaching events are likely to increase more in the next

69   decades/centuries

Biogeosciences
Discussions

EGU
Open Access

1   Introduction

Increasing atmospheric CO_2 at unprecedented rate since the industrial revolution, AD ~1850 and its consequences in terms of lowering of ocean pH called "Ocean acidification" has become a growing threat to many calcifying marine organisms (Doney et al., 2009; Hoegh-Guldberg et al., 2007). OA reduces carbonate saturation of seawater (Feely et al., 2004; Hoegh-Guldberg et al., 2007; Langdon and Atkinson, 2005; Orr et al., 2005)   which has adverse effects on calcifying marine organisms (Langdon and Atkinson, 2005). Atmosphere CO_2 has increased from ca. 280 ppm (Petit et al., 1999) since the beginning of industrial revolution (AD 1850) to ca. 410 ppm at present (https://www.esrl.noaa.gov/gmd/ccgg/trends/). About 20–30% of the anthropogenic CO_2 has been absorbed by ocean during the last century which resulted decrease in ocean pH by ca. 0.1 unit (Raven et al., 2005; Sabine et al., 2004). Model predictions shows that ocean pH is expected to reduce further by 0.2 to 0.3 unit by end of the 21st century, however, these predictions are associated with large uncertainties (Caldeira and Wickett, 2003; IPCC, 2007; Orr et al., 2001). In order to improve our current understanding about OA process and its future trend, it is important to have knowledge on spatio-temporal evolution of ocean pH. The longest instrumental records of past pH are available only from two stations i.e. Hawaiian Ocean Time Series (HOTS) (Dore et al., 2009) and Bermuda Atlantic Time Series (BATS) (Bates, 2007) stations in the Pacific and the Atlantic oceans respectively. However, these records are available only for the past three decades since AD 1984. Therefore, to have the records of ocean pH beyond the instrumental era, we have to rely on proxy records. Boron isotopes ($\delta^{11}B$) measured in marine carbonates show

93   promise as a reliable proxy for paleo-ocean pH (Foster and Rae, 2016; Hönisch et al.,

94   2004; Trotter et al., 2011). Further, boron isotopes of corals provide pH records

95   comparable to the resolution of instrumental records of the past few decades to

96   several centuries.

97   Boron has two naturally occurring stable isotopes, ^{10}B and ^{11}B with relative

98   abundance of 20% and 80% respectively. In seawater column, B behaves as a

99   conservative element with an average concentration of 4.5 ppm (Lee et al., 2010).

100   Boron isotope ratio is expressed in the form of delta notation relative to NIST-SRM-

101   951 (Catanzaro et al., 1970)

$$\delta^{11}B = \left(\frac{(^{11}B/^{10}B)_{Sample}}{(^{11}B/^{10}B)_{Standard}} - 1 \right) \times 1000 \qquad \textit{eq. (1)}$$

102   Dissolved boron in seawater exists in the form of two compounds, boric acid (B(OH)$_3$)

103   and borate ion (B(OH)$_4^-$). The relative abundance of these two compounds critically

104   depends on ocean pH (Dickson, 1990). The δ^{11}B of these compounds varies as a

105   function of pH, which is recorded in marine carbonates at the time of calcification

106   (Hemming and Hanson, 1992; Vengosh et al., 1991). When calcifying marine

107   organisms form their shells, they preferentially incorporate B(OH)$_4^-$ and hence the δ^{11}B

108   of the carbonates is similar to that of the B(OH)$_4^-$ in ambient seawater (Hemming and

109   Hanson, 1992). Following is the empirical relation to reconstruct pH of seawater using

110   δ^{11}B measured in marine carbonates, provided that there is no vital effect (species

111   related variations) (Zeebe and Wolf-Gladrow, 2001)

112   pH

113   $$= pK_B^* - \log\left(-\frac{\delta^{11}B_{SW} - \delta^{11}B_{Borate}}{\delta^{11}B_{SW} - {}^{11-10}K_B \times \delta^{11}B_{Borate} - 1000\,({}^{11-10}K_B - 1)} \right) \qquad eq\ (2)$$

114   Here, $\delta^{11}B_{sw}$ represents delta value of seawater (39.61‰; Foster et al. (2010)), pK_B^* is

115   dissociation constant of boric acid (8.597 at 25°C and 35 PSU salinity; Dickson

116   (1990)), $^{11\text{-}10}K_B$ is fractionation factor between $B(OH)_4^-$ and $B(OH)_3$ (1.0272; Klochko et

117   al. (2006)) and $\delta^{11}B_{borate}$ represents delta value of the sample.

118   Most of the earlier studies have focused on the reconstruction of paleo-pH

119   during the Quaternary glacial-interglacial periods and the Late Cenozoic era using $\delta^{11}B$

120   records of foraminifera (Hönisch and Hemming, 2005; Martínez-Botí et al., 2015;

121   Pearson and Palmer, 1999; Sanyal et al., 1997; Sanyal et al., 1995). However, similar

122   studies on shorter time scale (annual-decadal scale) based on coral records

123   particularly in the time scale of the Anthropocene are sparse. Boron isotopes have

124   been studied in corals from the Pacific and the Atlantic oceans (D'Olivo et al., 2015;

125   Fowell et al., 2018; Goodkin et al., 2015; Kubota et al., 2017; Liu et al., 2014; Pelejero

126   et al., 2005; Shinjo et al., 2013; Wei et al., 2009; Wei et al., 2015; Wu et al., 2018) to

127   reconstruct pH records of the past few decades to several centuries. In most of these

128   studies, it has been suggested that pH variability is mostly controlled by various

129   oceanographic factors such as upwelling, ocean circulation, river run-off and

130   productivity and therefore, making difficult to deconvolute the contribution of

131   anthropogenic pCO_2 forcing in modulating ocean pH. Further, several oceanographic

132   factors and their contributions are highly variable in space and time. In order to

133   improve our current understanding about recent trend of OA caused by anthropogenic

134   CO_2 during the past two centuries, it is important to have the knowledge on past pH

135   variability driven by oceanographic factors and their contributions.

136   In this study, we have made a comprehensive assessment of pH records

137   reconstructed using $\delta^{11}B$ of corals from the Pacific and the Atlantic oceans and

138   investigated forcing factors and their contributions to pH variability.

139   **2. pH records from the Pacific and the Atlantic Ocean corals**

140   We have compiled boron isotope ($\delta^{11}B$) derived pH records from the Pacific and

141   Atlantic oceans. In addition, we have also adopted a new approach to reconstruct pH

142   record based on theoretical calculation of the past records of carbonate system

143   parameters (pCO_2, total alkalinity (TA), sea surface temperature (SST) and salinity

144   (SSS)) from the same corals and using them into the CO2SYS program. In the

145   following sections, we have discussed about the pH records reconstructed using two

146   independent methods.

147   **2.1 $\delta^{11}B$ derived pH records**

148   We have compiled all the $\delta^{11}B$ records of corals from the Pacific and the Atlantic

149   oceans. To the best of our knowledge, total ten records with resolution of 1 – 5 years

150   are available in literature; however, no such record exists for the Indian Ocean (Fig. 1;

151   Table 1). For these records, boron isotope measurements in corals were performed

152   either by TIMS or MC-ICPMS instruments with analytical uncertainty better than ±

153   0.34‰ (± 2σ SD) which corresponds to the pH uncertainty of ~0.05. For all the records

154   compiled in this study, pH of the calcifying fluid (pH_{CF}) was calculated using equation

155   2. The values of $\delta^{11}B_{sw}$ (39.6‰; Foster et al. (2010)) and dissociation constants pK_B^*

156   (8.597 at 25°C and 35 PSU salinity; Dickson (1990)), $^{11\text{-}10}K_B$ (1.0272; Klochko et al.

157   (2006)) are used in equation 2. In order to compare these records, pH of the seawater

158   (pH_{SW}, total scale) for all the records was calculated using the calibration equation for

159   the coral species, *Porites cylindrica,* $pH_{SW} = (pH_{CF} - 4.72)/0.466$ (Fowell et al., 2018;

160   Liu et al., 2014; McCulloch et al., 2012; Trotter et al., 2011) (see the supplementary

161   data). The compilation of ten $\delta^{11}B$ records from the Pacific and the Atlantic Oceans

162   shows large variability; range between 26.27 - 20.82 ‰ which corresponds to pH_{SW}

163   range 8.40 - 7.63 (Figs. 2, 3 & Table 1). A LOESS fit (non-parametric fit) of these $\delta^{11}B$

164   records which is independent of data density show discernible decreasing trend since

165   the beginning of industrial era ~1850 AD, however, rapid declining trend was observed

166   since ~1970 AD (Fig. 2). Since $\delta^{11}B$ is linearly related to pH, decrease in $\delta^{11}B$ (Fig. 2)

167   corresponds to decrease in ocean pH.

168   In order to understand past ocean pH variability on a regional scale, $\delta^{11}B$

169   derived pH are grouped into four oceanic sectors (Fig. 1 & 3) based on the proximity of

170   these coral records i.e. Great Barrier Reef (GBR), South China Sea (SCS), North-

171   West Pacific and North-West Atlantic (Fig. 1 & 3). Four $\delta^{11}B$ derived pH records are

172   available from the South-West Pacific (GBR) (Fig. 3a) i.e. two are from the GBR

173   (D'Olivo et al., 2015; Wei et al., 2009) and another two from the Flinders reef (Pelejero

174   et al., 2005) and New Caledonia reef (Wu et al., 2018). The $\delta^{11}B$ records from the

175   GBR vary from 26.27 to 21.06 ‰ and its corresponding pH ranges from 8.40 to 7.67

176   (Fig. 3a). The $\delta^{11}B$ records from the SCS (Fig. 3b) vary from 26.00 to 20.82 ‰ and

177   corresponding pH ranges from 8.37 to 7.63 (Liu et al., 2014; Wei et al., 2015). The

178   records of $\delta^{11}B$ from the north-west Pacific varies from 25.02 to 22.10 ‰ and its

Biogeosciences
Discussions

179   corresponding pH ranges from 8.23 to 7.82 (Fig. 3c) (Kubota et al., 2017; Shinjo et al.,

180   2013). To the best of our knowledge, only two pH records are available from the

181   Sargasso Sea and the Mesoamerican Barrier Reef System (MBRS) in the Atlantic

182   Ocean (Fowell et al., 2018; Goodkin et al., 2015) of which $\delta^{11}B$ ranges from 25.36 to

183   22.70 ‰ and its corresponding pH ranges from 8.28 to 7.91 (Fig. 3d).

184

185   **2.2 Reconstruction of pH records using carbonate system parameters in**

186   **CO2SYS program**

187   We have adopted a novel approach to reconstruct paleo-pH of ocean based on the

188   past records of carbonate system parameters (hereafter, theoretical pH). Carbonate

189   system comprises of six parameters (pH, CO_2, $[CO_3^{2-}]$, $[HCO_3^-]$, TA and DIC) (Dickson

190   et al., 2007; Millero, 2006; Zeebe and Wolf-Gladrow, 2001). At any given two known

191   carbonate system parameters along with SST and SSS, we can theoretically calculate

192   other parameters. We have reconstructed theoretical pH using Matlab based CO2SYS

193   program (Van Heuven et al., 2011). For theoretical pH reconstruction, we have used

194   past records of SST, SSS, TA and pCO_2. Past SST and SSS were reconstructed

195   based on proxy records of Sr/Ca, Mg/Ca and $\delta^{18}O$ from the same corals in which $\delta^{11}B$

196   records are available. The details of the past SST, SSS and TA reconstructions are

197   provided in supplementary material (section S1 & Table S1). Such coral records are

198   available only from three sites i.e. GBR (Wei et al., 2009), SCS (Wei et al., 2015) and

199   Sargasso Sea (Goodkin et al., 2015). The reconstructed theoretical pH ranges from

200   8.05 - 8.16 in the GBR, 8.16 - 8.04 in the SCS and 8.19 - 8.09 in the Sargasso Sea.

201   Since the reconstructed parameters (SST, SSS and TA) are associated with

202   uncertainties, hence we did error propagation and estimated net uncertainty

203   associated with the theoretical pH (gray shade, Fig. 3) using Monte-Carlo error

204   propagation method in MATLAB (Wagener et al., 2001) (see supplementary material,

205   Section S2). We also performed sensitivity analysis of the parameters i.e. temperature,

206   salinity, pCO_2 and total alkalinity to the error associated with the pH reconstruction

207   using CO2SYS program (See supplementary material, Fig.S2).

208   Theoretical pH records show monotonic decreasing trend since ~ 1850 AD

209   which is consistent with that of atmospheric CO_2 forcing since the beginning of the

210   industrial era (Fig. 3). Variability in $\delta^{11}B$ derived pH records is larger than theoretical

211   pH in case of Pacific Ocean, whereas in case of Atlantic they mostly fall within the

212   error envelops (Fig. 3). This clearly indicates that contribution of atmospheric CO_2 and

213   physical parameters (SST and SSS) to the total pH variability are much lower

214   compared to other factors in the coral reef environments which are highly variable from

215   one reef to another in the Pacific. However, it is noteworthy to mention that in spite of

216   lower contribution of atmospheric CO_2 to pH, it shows discernable decreasing trend in

217   most of the records since ~1850 AD. We have compared theoretical pH and $\delta^{11}B$

218   derived pH records with model derived pH projections (Hartin et al., 2016) for the lower

219   latitude (<55° Latitude) for various representative concentration pathway (RCP)

220   scenarios. This shows that the theoretical pH records overall follow the historic record;

221   decrease in the ocean pH will be more severe in coming decades/century (Fig. 3e). It

222   is important to mention here that neither such proxy records nor long-term instrumental

223   records of ocean pH are available from the Indian Ocean.

224

Biogeosciences
Discussions

Open Access

EGU

3. Discussion

225

226   Ocean pH is influenced by multiple factors such as temperature (Dissard et al., 2012;

227   Reynaud et al., 2004), upwelling (Wei et al., 2015), ocean circulation (Pelejero et al.,

228   2005; Wei et al., 2009), precipitation (Deng et al., 2013; Liu et al., 2014), run off

229   (D'Olivo et al., 2015), nutrients supply and productivity (Bates et al., 2010; Goodkin et

230   al., 2015). Therefore, the knowledge on spatio-temporal evolution of ocean pH and its

231   link to ocean-climate oscillations are important for recognizing individual factors and

232   their relative contribution. To identify the regions that come under the influence of

233   known ocean-climate oscillations, spatial correlation of temperature and precipitation

234   were performed with the indices of dominant climate oscillations ((El-Niño southern

235   oscillation (ENSO) and Pacific decadal oscillation (PDO)) using online software

236   "climate analyzer" (http://cci-reanalyzer.org/reanalysis/monthly_correl/). The regions of

237   significant (90% significance level) correlations are highlighted in color bands (Fig. 4(I)

238   a, b, c & d). Similarly, spatial correlation analysis was performed with Atlantic multi-

239   decadal oscillation (AMO) and North Atlantic Oscillation (NAO) which are known as

240   dominant oscillations in the Atlantic (Fig. 4(II) a, b, c & d). Overall, we observe that all

241   the coral sites in this study come under the influence of ENSO and PDO in the Pacific

242   and AMO and NAO in the Atlantic though the modulation of SST, precipitations, run-off

243   and oceanographic parameters nutrient supply, upwelling and circulations and

244   therefore responsible for changes in ocean pH.

245   As $\delta^{11}B$ variability is the direct response of ocean pH and therefore,

246   periodicities determined based on power spectrum analysis of $\delta^{11}B$ records enable us

247   to establish linkages between the pH variability and the specific oscillations i.e. ENSO

Biogeosciences

Discussions

Open Access

EGU

248 and PDO in the Pacific and AMO and NAO in the Atlantic. Further, wavelet analyses of

249 these records decompose the δ^{11}B time series into time and frequency space and

250 highlights in color bands (Fig. 4(I) & 4(II)). All the periodicities observed in δ^{11}B records

251 and ocean-climate indices are listed in table 2 including the climate indices

252 (supplementary Fig. S3). In the following sections we have discussed about the

253 specific oscillation that registered in the δ^{11}B records and how they evolved in the past.

254 **3.1 δ^{11}B variability in the Pacific and Atlantic oceans and their link to ocean-**

255 **climate oscillations**

256 The δ^{11}B records from the South China Sea (SCS) (Wei et al., 2015) and the Guam

257 Island in north-west Pacific (Shinjo et al., 2013) show dominant periodicities of ~3, ~6

258 and ~17 years (Fig. 4(I) e, f; Table 2). Though these two coral reefs represent different

259 oceanic environments (SCS represents coastal environment and the Guam Island

260 represents open ocean environment), they exhibit common periodicities of ~3 years

261 and ~6 years (Fig. 4(I) e, f). However, another record (1825 – 2000 AD) from the

262 proximity (Liu et al., 2014) in coastal region of SCS (Fig. 3b) does not show any

263 significant periodicity. This could be due to lower resolution (4 years) of this record and

264 hence, the high frequency oscillations do not get captured in the power spectrum

265 analysis. Two records from the central GBR in the South Pacific (D'Olivo et al., 2015;

266 Wei et al., 2009) have shown dominant periodicities of ~3, ~5, ~10 and ~23 years (Fig.

267 4(I) g & h; Table 2). Flinders reef in the south-western Pacific (Pelejero et al., 2005),

268 shows dominant periodicities of ~10, ~16 and ~50 years (Fig. 4(I) i). New Caledonia is

269 one of the longest records with annual resolution exhibits periodicities of ~5.4, ~7, ~13

270   and ~30 years (Fig. 4(I) j). Most of the frequencies captured in the analysis fall within

271   the band of ENSO (2 – 8 years) and few of them are within the band of PDO (decadal

272   scale) respectively (Table 2). ENSO has strong influence on upwelling in the Pacific

273   (Inoue et al., 2001; Ishii et al., 2009; Sutton et al., 2014; Takahashi et al., 2003) and

274   nutrient supply to the coastal regions of the SCS through rivers run-off. The PDO,

275   another dominant ocean-climate mode is known to influence physical and

276   biogeochemical conditions and thereby influence ocean pH at decadal time scale

277   (D'Olivo et al., 2015; Pelejero et al., 2005; Wei et al., 2009; Wu et al., 2018).

278   The δ^{11}B record from the Sargasso Sea (Goodkin et al., 2015) shows dominant

279   periodicities of ~5, ~7, and ~14 years (Fig. 4(II) e; Table 2). Further wavelet analysis

280   shows dominant periodicities at 4 - 8 year band throughout the last two centuries and

281   14 - 20 year band during AD 1870 - 1970. The δ^{11}B record from the MBRS shows

282   periodicities of ~7, ~17 and ~25 years (Fig. 4(II) f, g). The lower periodicities less than

283   10 years are similar to that of NAO and therefore highlight the role of NAO in

284   modulating ocean pH at annual-decadal scale (Supplementary Fig. S3). The longer

285   periodicities at decadal scale (~10 years and 25 years) captured in the spectrum

286   analysis are similar to that of AMO and hence indicates its role in modulating ocean

287   pH (Supplementary Fig. S3).

288   In conclusion, our analysis clearly indicates that ocean pH is influenced by

289   oceanographic factors modulated by dominant ocean-climate modes i.e. ENSO and

290   PDO in the Pacific and NAO and AMO in the Atlantic oceans.

3. Identification of forcing factors and their contribution to pH variability

Atmospheric CO_2 and oceanographic factors driven by ocean-climate oscillations are known to influence ocean pH, however, their relative contribution are not well constrained. Therefore, it is indeed important to identify dominant factors and quantify their relative role in controlling pH variability in the Pacific and the Atlantic oceans. For this purpose, we have employed statistical method "Principal Component Analysis (PCA)" to all the available $\delta^{11}B$ records using excel based XLSTAT® program (https://www.xlstat.com). For this analysis, at least four records are required for better statistical control and therefore, we restricted this analysis up to the Pacific records within the time slice 1950 – 2004 AD in which the highest numbers of records (Fig. 5a) are available (Fig. 2). PCA is a statistical method which reduces multi-dimensional complex dataset consisting of large number of inter-related variables into few simpler variables without significant loss of original information (Abdi and Williams, 2010; Meglen, 1992). Further, PCA also recognizes pattern and explain large dataset with interrelated variables. The results obtained from the PCA analysis is shown in Fig. 5a, b & c. The first (PC1) and second principal components (PC2) explain 26.2% and 16.7% of the total variability respectively (Fig. 5a).

The overall trend of the PC1 is consistent with the increasing trend of atmospheric CO_2; (Fig. 5b). Hence, we recognize PC1 as a factor that representing atmospheric CO_2 forcing. In earlier studies, it has been reported that atmospheric CO_2 forcing contributes less than 10% of the total pH variability in the Atlantic (Goodkin et al., 2015), which is lower than the estimate (~26%) in the Pacific Ocean. Power spectrum analysis of the PC2 shows significant periodicities of ~20 and ~4.5 years

314   which are similar to that of PDO and ENSO respectively and therefore we recognize

315   PC2 as an oceanographic factor. In conclusion, our investigation reveals that

316   atmospheric CO_2 forcing together with oceanographic factors (ENSO and PDO driven

317   changes) can explain maximum up to 43% of the total pH variability in the Pacific. It is

318   noteworthy to highlight here that remaining variability of 57% could not be explained by

319   the forcing factors mentioned above. Hence, we invoke metabolic processes of corals

320   and changes in micro-environment within the corals reefs might play an important role

321   on boron isotope fractionation, and, therefore, highlights the need for further

322   investigation. Few laboratory experiments and field studies have suggested that micro-

323   environment in corals reefs and metabolic processes play an important role in

324   regulating pH of the calcifying fluid (CF) (McCulloch et al., 2012; Wall et al., 2016).

325   Corals elevate pH of the CF region to facilitate calcification, called pH-upregulation (Al-

326   Horani et al., 2003; Gattuso et al., 1999; McConnaughey and Whelan, 1997;

327   McCulloch et al., 2012; Wall et al., 2016) and hence record the pH of the CF region

328   rather than the ambient seawater (Allison et al., 2010; Anagnostou et al., 2012;

329   McCulloch et al., 2017). Therefore, the species specific pH-upregulation is one of the

330   important caveats that need to be considered while reconstructing ocean pH using

331    $\delta^{11}B$ records. To circumvent this problem, species specific calibration is indeed

332   important for pH reconstruction using $\delta^{11}B$ records (McCulloch et al., 2012; Trotter et

333   al., 2011).

334   We compared PC1 with the instrumental record of annual mean ocean pH from

335   the HOTS time series station in the Pacific which is available since 1988. Overall, they

336   follow similar trend (Fig. 6a), however, scatter plot shows two distinct trends

Biogeosciences
Discussions

Open Access

337   compatible with linear fits (Fig. 6b). This indicates two dominant processes that control

338   pH variability at HOTS station. We have reconstructed two pH records corresponding

339   to the PC1 using these regressions equations. The PC1 derived pH record (blue

340   curve) follow closely with the trend of theoretical pH curve whereas other (red-curve)

341   shows large off-set. Therefore, the PC1 derived blue curve corresponds to the pH

342   curve due to changes in atmospheric CO_2.

343   PC2 is a factor that represents the Pacific oscillations i.e. ENSO and PDO as

344   discussed above. It is important to understand how ENSO and PDO individually

345   contributed to the pH variability. To infer about how these two modes individually

346   influenced pH variability in the Pacific Ocean, we have deconvolute the signals of

347   ENSO and PDO from the PC2 time series by filtering them at 4-5 years and 18-20

348   years bands respectively (Fig. 7b, & c). It is noteworthy to observe that PC2 at ENSO

349   band shows higher amplitude variability after ~1970 AD whereas at PDO band does

350   not show any discernable changes. To quantify ENSO driven pH variability, we have

351   estimated scaled average variance which shows almost fivefold increase during 1980

352   – 2004 compared to that of previous decades 1950 – 1980 (Fig. 7b). Since many of

353   the historical coral bleaching events are often associated with extreme El-Niño events

354   (Hoegh-Guldberg, 1999; Hughes et al., 2018; Kelmo et al., 2014), we have compared

355   ENSO signal with the reported global coral bleaching events (Hughes et al., 2018) .

356   The trend of the coral bleaching events follows almost similar to the trend of the

357   variance of ENSO signal (Fig.7 b & d). This indicates that large pH variability and

358   some of extensive corals bleaching events are associated with extreme ENSO events.

359   Modeling studies suggested that in the backdrop of the increasing greenhouse

Biogeosciences
Discussions
Open Access
EGU

360   warming, frequencies and amplitude of ENSO and associated extreme events are

361   expected to increase in the next decades (Cai et al., 2014; Cai et al., 2012), therefore,

362   frequency of coral bleaching events and its magnitude particularly in the Pacific Ocean

363   are also expected to increase in future decades/centuries (Ainsworth et al., 2016;

364   Kwiatkowski et al., 2015).

365   **4. Conclusions**

366   In this study, we have assessed published high resolution records of $\delta^{11}B$

367   derived pH from the Pacific and the Atlantic Ocean corals to decipher the contribution

368   of atmospheric CO_2 forcing vis-à-vis oceanographic factors to pH variability and

369   changes during the past two centuries. This study based on the large data sets

370   provide a holistic picture of the pH variability and relative role of individual forcing

371   factors in the Pacific and the Atlantic oceans. Our specific observations and findings

372   are concluded below

373   i.   Compilation of $\delta^{11}B$ records shows overall decreasing trend during the past two

374   centuries with more rapid decrease since ~1970 AD. This observation is

375   consistent with the concomitant rise of atmospheric CO_2 since the industrial

376   revolution ~1850 AD.

377   ii.   pH variability in the Pacific ocean is larger than that of the Atlantic ocean which

378   suggests dominant role of ENSO and PDO in modulating ocean pH.

379   iii. Our investigations based on principal component analysis of the $\delta^{11}B$ derived

380   pH records reveals ~26% and ~17% variability in the Pacific ocean pH are

381   explained by atmospheric CO_2 and Pacific ocean-climate oscillations

382   respectively. Remaining large unexplained variability (57%) might be related to

383   metabolic processes and micro-environmental changes of the corals reefs.

384   Therefore, we highlight the need for more detailed investigation of boron

385   isotope fractions and its relations to specific metabolic processes and micro-

386   environmental changes based on laboratory experiments and field studies in

387   the corals reefs.

388 iv. We have estimated pH reduction in the Pacific Ocean by 0.5 unit due to

389   anthropogenic CO_2 forcing; rise of atmospheric CO_2 from 310 to 380 ppm

390   during 1950 – 2004.

391 v. ENSO driven pH variability shows large increase during 1980 – 2004 compared

392   to previous decades (1950 – 1980). This observation is consistent with the

393   reported global coral bleaching events. This indicates thermal stress associated

394   with extreme ENSO events could be responsible for coral bleaching events.
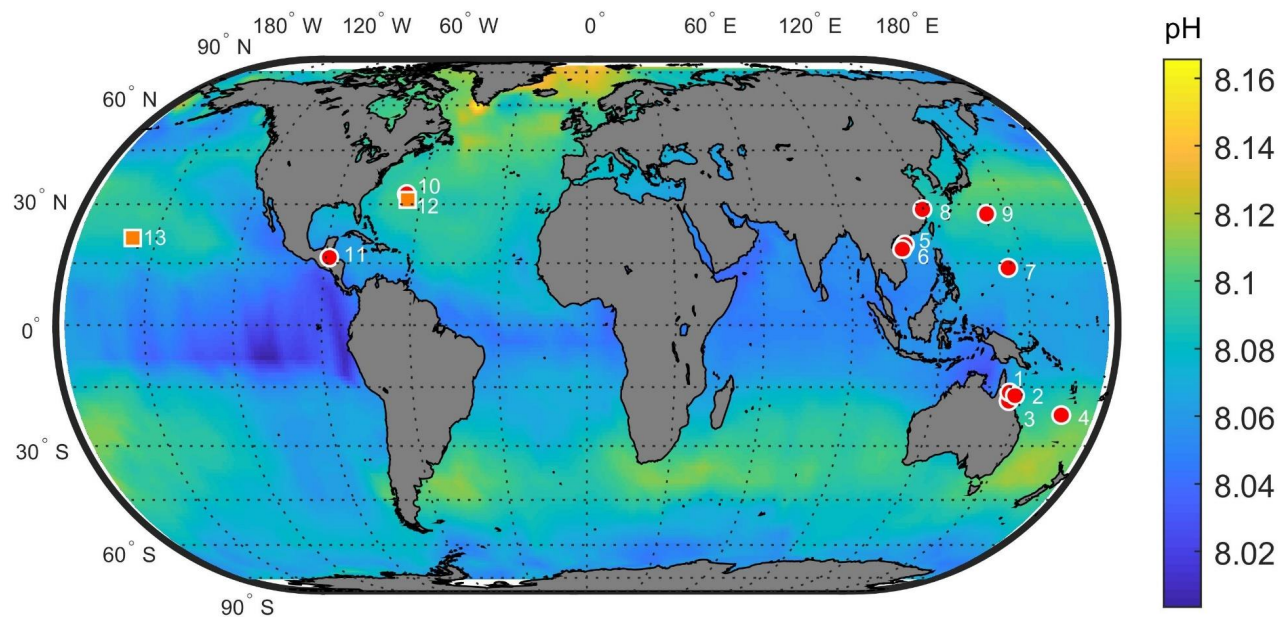
395 vi. Considering the model based prediction of the extreme events associated with

396   ENSO in the backdrop of the increasing global warming, coral bleaching events

397   are likely to increase in future decades/centuries.

398

403

1. Wei et al., 2009 2. Pelejero et al., 2005 3. D'Olivo et al., 2015 4. Wu et al., 2018 5. Wei et al., 2015 6. Liu et al., 2014
7. Shinjo et al., 2013   8 & 9. Kubota et al., 2017 10. Goodkin et al., 2015 11. Fowell et al., 2018 12. BATS   13. HOTS

404

405   Figure 1: Location of the coral reefs from where δ¹¹B records are available (shown in red circle). Square show in-situ pH time series stations i.e.

406   HOTS in the Pacific and BATS in the Atlantic. Color band represent pH of the surface ocean from Takahashi et al. (2014).

19
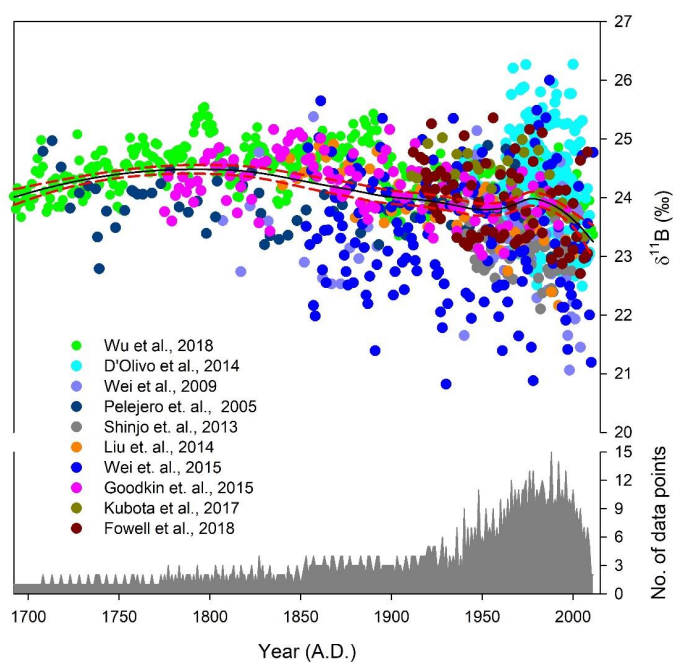
407

408   Figure 2: The $\delta^{11}B$ records from the Pacific and the Atlantic Ocean corals. The black line represent the LOESS fit of all the data. Dashed red line represent

409   the 95 percent confidence interval of the fit. Confidence band of the LOESS fit was determined using bootstrap in Matlab. The lower panel represents data

410   density; the number of $\delta^{11}B$ data points for each year.

20

Biogeosciences
Discussions

Open Access

EGU
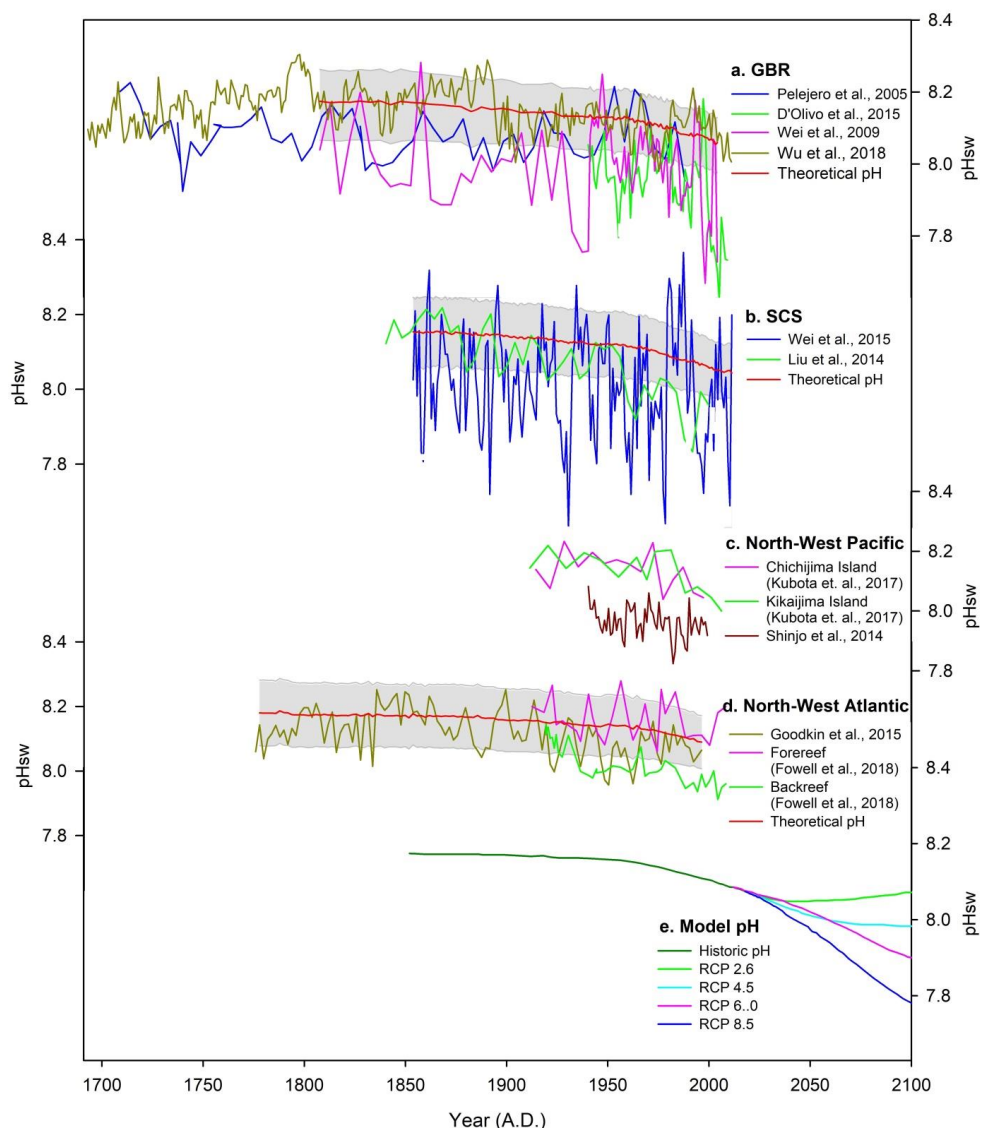
411
412
413   Figure 3: The δ^{11}B derived pH records from the Pacific: (a) GBR, (b) SCS, (c) North-West Pacific and

414   from the Atlantic: (d) North West Atlantic. Red color solid curves represent theoretical pH for the sites

415   GBR, SCS and North-West Atlantic. Reconstruction of theoretical pH is discussed in section 2.2. Gray

416   envelops represents uncertainty in the theoretical pH reconstruction. δ^{11}B derived pH records and

417   theoretical pH are compared with the Hector model derived pH projections (Hartin et al., 2016) of low

418   latitude (<55° Latitude) for various representative concentration pathway (RCP) scenarios.

Biogeosciences
Discussions

Open Access

419
420
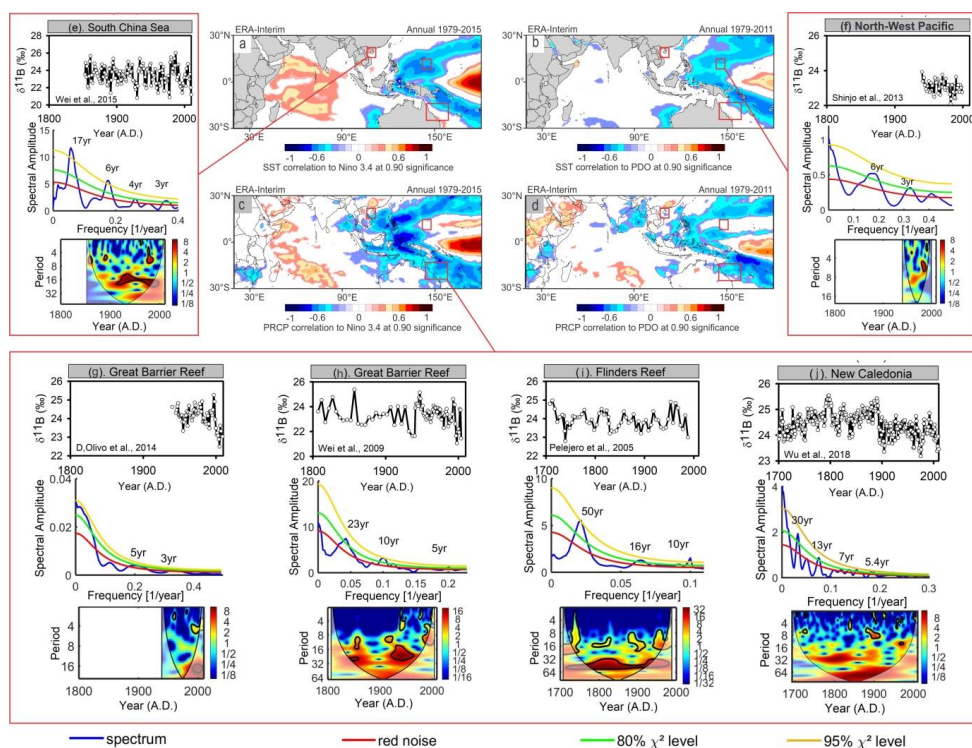
Figure 4(I): Spatial correlation between records of (a) SST and Niño 3.4, (b) SST and PDO, (c) precipitation and Niño 3.4, (d) precipitation and PDO indices. Reanalysis ERA-Interim data of SST and precipitation records are used in the spatial correlation analysis. The regions of significant correlation are highlighted in color code at 90% significance level. Spatial correlation plot was generated from Climate Reanalyzer (http://cci-reanalyzer.org). Red colour square indicates the locations of the coral sites in the Pacific Ocean. The δ^{11}B records and their spectral and wavelet analysis from the sites: (e) SCS (Wei et al., 2015), (f) Guam Island (Shinjo et al., 2013), (g) GBR (D'Olivo et al., 2015), (h) GBR (Wei et al., 2009), (i) Flinders Reef (Pelejero et al., 2005) and (j) New Caledonia (Wu et al., 2018). Spectrum analysis were performed using MATLAB based Redfit program (Schulz and Mudelsee, 2002). Wavelet analysis decomposes time series in time and frequency space. Thick contour represents 5% significance level against red noise. The thin solid lines represent cone of influence. The color band highlights how periodicities vary with time. Wavelet analysis was performed using online MATLAB codes taken from Torrence and Compo (1998). The wavelet

22

434   analyses were performed using online available MATLAB codes from Grinsted et al. (2004)

435   (http://grinsted.github.io/wavelet-coherence/).

436
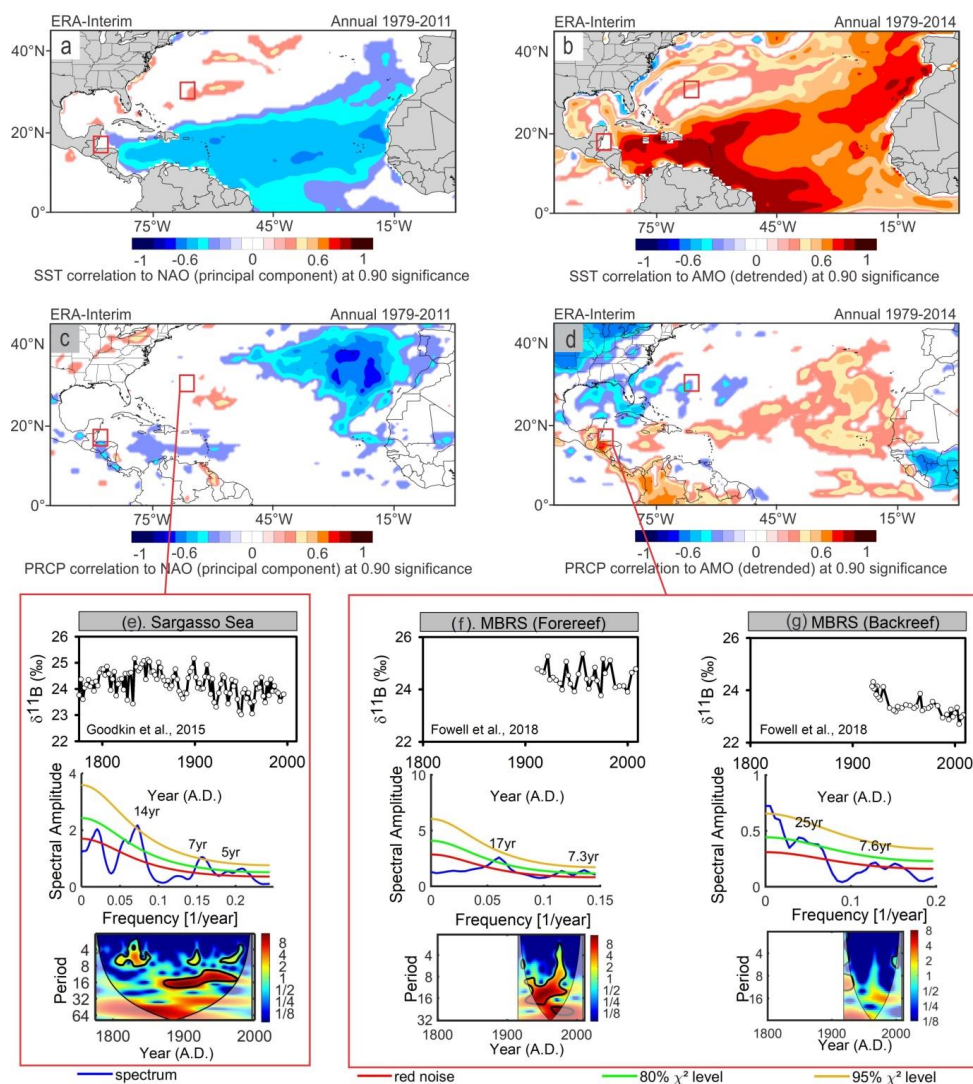
437

438

439   Figure   4(II): Spatial correlation between the records of (a) SST and NAO, (b) SST and AMO, (c)

440   precipitation and NAO, (d) precipitation and AMO. The δ¹¹B records and their power spectrum and

441   wavelet analysis were performed for the sites: (e) Sargasso Sea (Goodkin et al., 2015) and (f & j)

442   MBRS (Fowell et al., 2018).

443
444
445
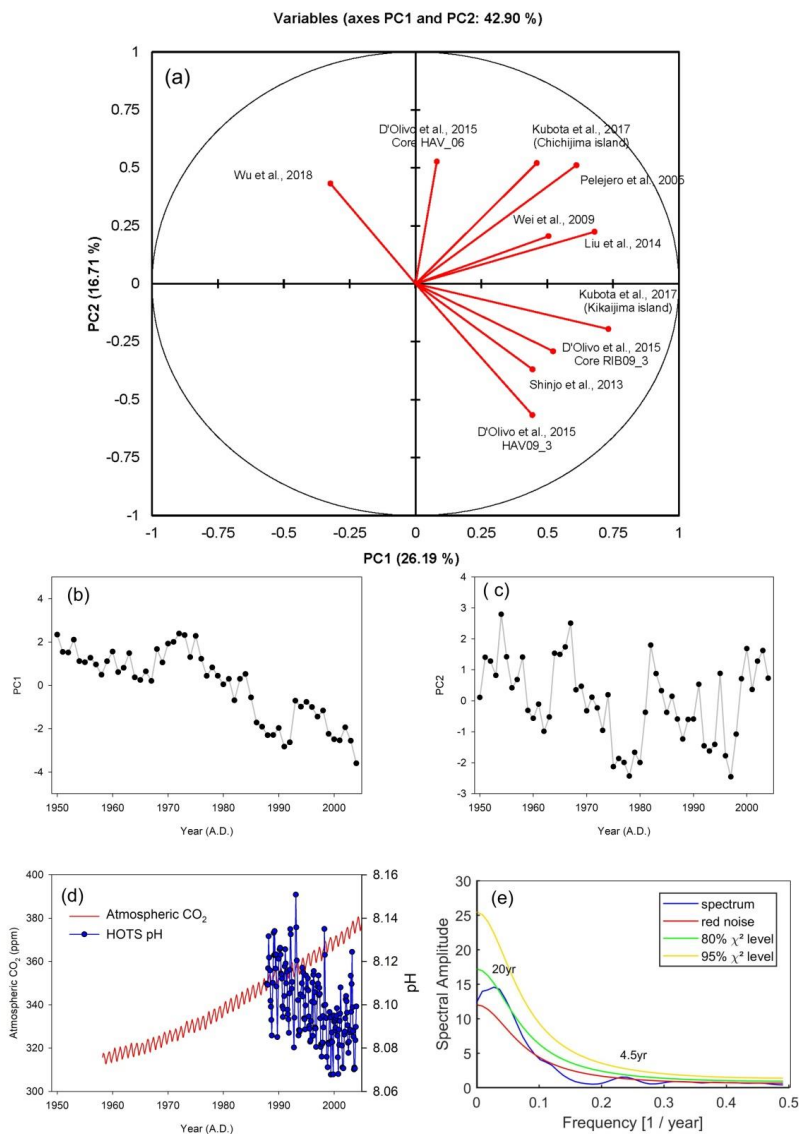
Figure 5:   Biplot of principal components PC1 vs. PC2. The vectors length and directions show

correlation between the factors and variables. PC1 and PC2 components explain ~43 % of the total

variability in $\delta^{11}B$ records from the Pacific. Records of (b) first principal component (PC1 score) and

(c) second principal component (PC2) derived from the principal component analysis of all the pacific

records of $\delta^{11}B$ (1950 – 2004 AD). (d) Instrumental records of atmospheric CO_2 (red curve)

24

452   (https://www.esrl.noaa.gov/gmd/ccgg/trends/) and pH records (blue line) from the time series station

453   HOTS in the Pacific Ocean. (e) Power spectrum analysis of PC2 record. This shows significant (80%

454   χ2 level) periodicities of 4.5 years and 20 years.

455
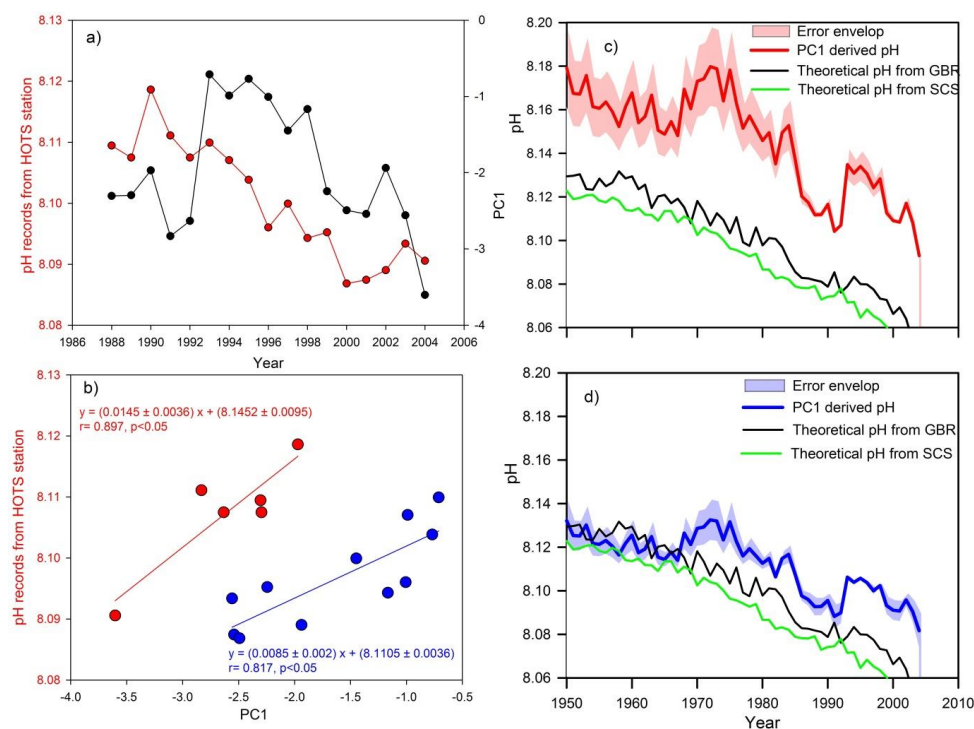
Figure: 6 a) Annual mean pH record from the HOTS station (1988 – 2004) is compared with PC1. (b)

PC1 record is plotted with pH record from HOTS station (1988 – 2004). Based on the distribution of

the data, two distinct trends are identified. These trends are compatible with linear fits with significant

correlations. (c & d) pH was reconstructed based the PC1 time series in the regression equations.

Solid (red and blue lines) represent mean pH and shade represents uncertainty associated with the

mean (2σ). Black and green line represent the theoretical pH for GBR and SCS regions respectively.

Biogeosciences
Discussions

Open Access

EGU
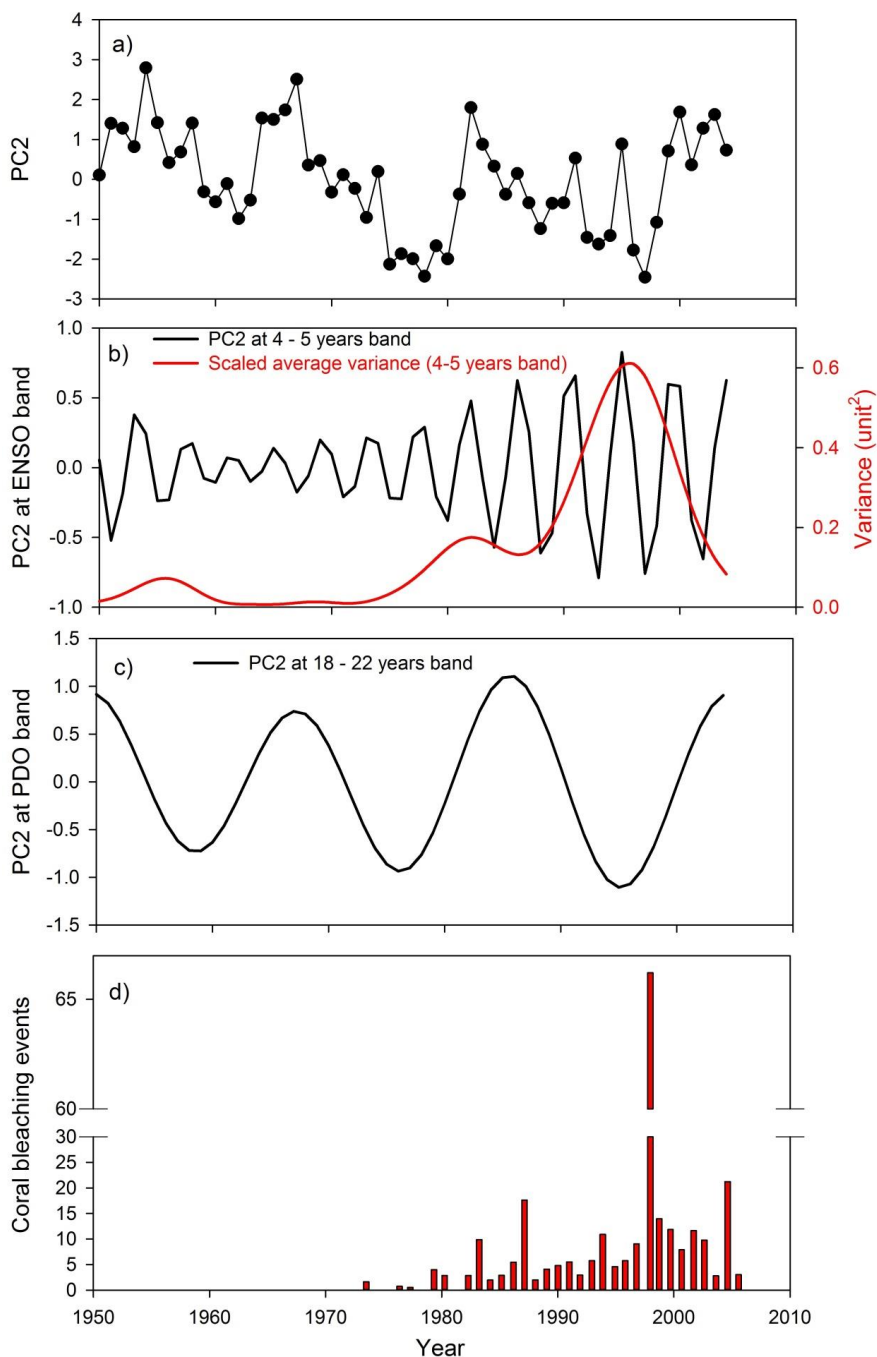
Figure 7: a) PC2 time series and b) extracted signal of ENSO at 4 – 5 years band and c) PDO signal

at 18 – 22 years band. The amplitude of the ENSO signal shows large increase after 1970 d) Number

of coral bleaching events after Hughes et al. (2018).

Biogeosciences
Discussions

466   Table 1: Details of published δ^{11}B records from Pacific and Atlantic Ocean

Location	Latitude, Longitude	δ^{11}B (‰) range (min – max)	pH range (min – max)	Boron isotope measurement	Time span (Years)	Resolution (Year)	Coral type	References
Pacific Ocean								
Great Barrier Reef	-18.84, 146.53	22.49 – 26.27	7.88 – 8.40	TIMS, MC-ICPMS	1940-2009	1	*Porites sp.*	D'Olivo et. al., 2015
Great Barrier Reef	-16.68, 146.12	21.06 – 25.38	7.67 – 8.28	TIMS	1807-2004	1, 5	*Porites sp.*	Wei et. al., 2009
Flinders Reef	-17.5, 148.3	22.79 – 24.97	7.92 – 8.23	TIMS	1781-1990	5	*Porites sp.*	Pelejero et al., 2005
New Caledonia	-22.21, 166.15	23.18 – 25.54	7.98 – 8.30	MC-ICPMS	1692-2011	1	*Diploastrea heliopora*	Wu et al., 2018
South China Sea	19.283, 110.65	20.82 – 26.00	7.63 – 8.37	TIMS	1853-2011	1	*Porites sp.*	Wei et. al., 2015
South China Sea	18.2, 109.499	22.16 – 24.91	7.83 – 8.22	MC-ICPMS	1840-2000	4	*Porites sp.*	Liu et. al., 2014
Guam Island	13.6, 144.80	22.10 – 23.92	7.82 – 8.08	MC-ICPMS	1940-1999	1	*Porites sp.*	Shinjo et. al., 2013
Kikaijima and Chichijima island	28.3, 130.0 27.1, 142.2	23.33 – 25.02	8.00 – 8.23	MC-ICPMS	1910-2007	5	*Porites sp.*	Kubota et.al., 2017
Atlantic Ocean								
Sargasso Sea	32.318, -64.717	23.02 – 25.16	7.96 – 8.25	MC-ICPMS	1775-1996	2	*Diploastrea heliopora*	Goodkin et. al., 2015
Belize Mesoamerican Barrier Reef	16.137, -88.252 16.140, -88.260	22.70 – 25.36	7.91 – 8.28	MC-ICPMS	1912-2008	1-6	*Siderastrea siderea*	Fowell et al., 2018

467
468
469
470
471
472
473
474
475
476

477
478   Table 2: Periodicities in δ^{11}B and climate indices
479

Location / Indices	Periodicities			References
	Low	Intermediate	High	
Great Barrier Reef	3, 5			D'Olivo et al., 2015
Great Barrier Reef	5	10	23	Wei et al., 2009
Flinders Reef		10, 16	50	Pelejero et al., 2005
New Caledonia	5.4, 7	13	30	Wu et al., 2018
South China Sea	3, 4, 6	17		Wei et al., 2015
Guam Island	3, 6			Shinjo et al., 2013
Sargasso Sea	5, 7	14		Goodkin et al., 2015
MBRS	7.3, 7.6	17	25	Fowell el al., 2018
Climate indices				
ENSO	2.4, 2.8, 3.6, 5.6			
PDO	3.3, 6	20	40	
NAO	1.5, 7.6			
AMO	5.7	10.5	23.8	

480
481
482 **References:**

483 Abdi, H. and Williams, L. J.: Principal component analysis, Wiley Interdisciplinary Reviews:

484   Computational Statistics, 2, 433-459, 2010.

485 Ainsworth, T. D., Heron, S. F., Ortiz, J. C., Mumby, P. J., Grech, A., Ogawa, D., Eakin, C.

486   M., and Leggat, W.: Climate change disables coral bleaching protection on the Great

487   Barrier Reef, Science, 352, 338-342, 2016.

488 Al-Horani, F. A., Al-Moghrabi, S. M., and de Beer, D.: The mechanism of calcification and its

489   relation to photosynthesis and respiration in the scleractinian coral Galaxea

490   fascicularis, Marine Biology, 142, 419-426, 2003.

491 Allison, N., Finch, A. A., and EIMF: $\delta^{11}B$, Sr, Mg and B in a modern Porites coral: the

492   relationship between calcification site pH and skeletal chemistry, Geochimica et

493   Cosmochimica Acta, 74, 1790-1800, 2010.

494 Anagnostou, E., Huang, K. F., You, C. F., Sikes, E. L., and Sherrell, R. M.: Evaluation of

495   boron isotope ratio as a pH proxy in the deep sea coral Desmophyllum dianthus:

496   Evidence of physiological pH adjustment, Earth and Planetary Science Letters, 349-

497   350, 251-260, 2012.

498 Bates, N. R.: Interannual variability of the oceanic CO_2 sink in the subtropical gyre of the

499   North Atlantic Ocean over the last 2 decades, Journal of Geophysical Research:

500   Oceans, 112, C09013, 2007.

501 Bates, N. R., Amat, A., and Andersson, A. J.: Feedbacks and responses of coral calcification

502   on the Bermuda reef system to seasonal changes in biological processes and ocean

503   acidification, Biogeosciences, 7, 2509-2530, 2010.

504 Cai, W., Borlace, S., Lengaigne, M., van Rensch, P., Collins, M., Vecchi, G., Timmermann,

505   A., Santoso, A., McPhaden, M. J., Wu, L., England, M. H., Wang, G., Guilyardi, E., and

506   Jin, F.-F.: Increasing frequency of extreme El Niño events due to greenhouse

507   warming, Nature Climate Change, 4, 111, 2014.

508   Cai, W., Lengaigne, M., Borlace, S., Collins, M., Cowan, T., McPhaden, M. J., Timmermann,

509   A., Power, S., Brown, J., Menkes, C., Ngari, A., Vincent, E. M., and Widlansky, M. J.:

510   More extreme swings of the South Pacific convergence zone due to greenhouse

511   warming, Nature, 488, 365, 2012.

512   Caldeira, K. and Wickett, M. E.: Anthropogenic carbon and ocean pH, Nature, 425, 365-365,

513   2003.

514   Catanzaro, E., Champion, C., Garner, E., Marinenko, G., Sappen-field, K., and Shields, W.:

515   Boric acid: isotopic and assay standard reference materials, National Bureau of

516   Standards (USA), Spec. Publ. 260–17, 1–70, 1970.

517   D'Olivo, J. P., McCulloch, M. T., Eggins, S. M., and Trotter, J.: Coral records of reef-water

518   pH across the central Great Barrier Reef, Australia: assessing the influence of river

519   runoff on inshore reefs, Biogeosciences, 12, 1223-1236, 2015.

520   Deng, W., Wei, G., Xie, L., Ke, T., Wang, Z., Zeng, T., and Liu, Y.: Variations in the Pacific

521   Decadal Oscillation since 1853 in a coral record from the northern South China Sea,

522   Journal of Geophysical Research: Oceans, 118, 2358-2366, 2013.

523   Dickson, A. G.: Thermodynamics of the dissociation of boric acid in synthetic seawater from

524   273.15 to 318.15 K, Deep Sea Research Part A. Oceanographic Research Papers, 37,

525   755-766, 1990.

526   Dickson, A. G., L., S. C., and Christian, J. R.: Guide to best practices for ocean CO_2

527   measurements, PICES Special Publication, 2007.

528   Dissard, D., Douville, E., Reynaud, S., Juillet-Leclerc, A., Montagna, P., Louvat, P., and

529   McCulloch, M.: Light and temperature effects on $\delta^{11}B$ and B/Ca ratios of the

530   zooxanthellate coral Acropora sp.: results from culturing experiments, Biogeosciences,

531   9, 4589-4605, 2012.

532   Doney, S. C., Fabry, V. J., Feely, R. A., and Kleypas, J. A.: Ocean acidification: the other

533   CO_2 problem, Annual review of marine science, 1, 169-192, 2009.

534   Dore, J. E., Lukas, R., Sadler, D. W., Church, M. J., and Karl, D. M.: Physical and
535   biogeochemical modulation of ocean acidification in the central North Pacific,
536   Proceedings of the National Academy of Sciences of the United States of America,
537   106, 12235-12240, 2009.
538   Feely, R. A., Sabine, C. L., Lee, K., Berelson, W., Kleypas, J., Fabry, V. J., and Millero, F. J.:
539   Impact of Anthropogenic CO_2 on the $CaCO_3$ System in the Oceans, Science, 305, 362-
540   366, 2004.
541   Foster, G. L., Pogge von Strandmann, P. A. E., and Rae, J. W. B.: Boron and magnesium
542   isotopic composition of seawater, Geochemistry, Geophysics, Geosystems, 11,
543   Q08015, 2010.
544   Foster, G. L. and Rae, J. W. B.: Reconstructing Ocean pH with Boron Isotopes in
545   Foraminifera, Annual Review of Earth and Planetary Sciences, 44, 207-237, 2016.
546   Fowell, S. E., Foster, G. L., Ries, J. B., Castillo, K. D., Vega, E., Tyrrell, T., Donald, H. K.,
547   and Chalk, T. B.: Historical Trends in pH and Carbonate Biogeochemistry on the
548   Belize Mesoamerican Barrier Reef System, Geophysical Research Letters, 45, 3228-
549   3237, 2018.
550   Gattuso, J. P., Allemand, D., and Frankignoulle, M.: Photosynthesis and calcification at
551   cellular, organismal and community levels in coral reefs: a review on interactions and
552   control by carbonate chemistry, Am. Zool., 39, 160–183, 1999.
553   Goodkin, N. F., Wang, B.-S., You, C.-F., Hughen, K. A., Grumet-Prouty, N., Bates, N. R.,
554   and Doney, S. C.: Ocean circulation and biogeochemistry moderate interannual and
555   decadal surface water pH changes in the Sargasso Sea, Geophysical Research
556   Letters, 42, 4931-4939, 2015.
557   Grinsted, A., Moore, J. C., and Jevrejeva, S.: Application of the cross wavelet transform and
558   wavelet coherence to geophysical time series, Nonlin. Processes Geophys., 11, 561-
559   566, 2004.

560   Hartin, C. A., Bond-Lamberty, B., Patel, P., and Mundra, A.: Ocean acidification over the

561   next three centuries using a simple global climate carbon-cycle model: projections and

562   sensitivities, Biogeosciences, 13, 4329-4342, 2016.

563   Hemming, N. G. and Hanson, G. N.: Boron isotopic composition and concentration in

564   modern marine carbonates, Geochimica et Cosmochimica Acta, 56, 537-543, 1992.

565   Hoegh-Guldberg, Mumby, P. J., Hooten, A. J., Steneck, R. S., Greenfield, P., Gomez, E.,

566   Harvell, C. D., Sale, P. F., Edwards, A. J., Caldeira, K., Knowlton, N., Eakin, C. M.,

567   Iglesias-Prieto, R., Muthiga, N., Bradbury, R. H., Dubi, A., and Hatziolos, M. E.: Coral

568   Reefs Under Rapid Climate Change and Ocean Acidification, Science, 318, 1737-

569   1742, 2007.

570   Hoegh-Guldberg, O.: Climate change, coral bleaching and the future of the world's coral

571   reefs, Marine and Freshwater Research, 50, 839-866, 1999.

572   Hönisch, B. and Hemming, N. G.: Surface ocean pH response to variations in pCO2 through

573   two full glacial cycles, Earth and Planetary Science Letters, 236, 305-314, 2005.

574   Hönisch, B., Hemming, N. G., Grottoli, A. G., Amat, A., Hanson, G. N., and Bijma, J.:

575   Assessing scleractinian corals as recorders for paleo-pH: Empirical calibration and

576   vital effects, Geochimica et Cosmochimica Acta, 68, 3675-3685, 2004.

577   Hughes, T. P., Anderson, K. D., Connolly, S. R., Heron, S. F., Kerry, J. T., Lough, J. M.,

578   Baird, A. H., Baum, J. K., Berumen, M. L., Bridge, T. C., Claar, D. C., Eakin, C. M.,

579   Gilmour, J. P., Graham, N. A. J., Harrison, H., Hobbs, J.-P. A., Hoey, A. S.,

580   Hoogenboom, M., Lowe, R. J., McCulloch, M. T., Pandolfi, J. M., Pratchett, M.,

581   Schoepf, V., Torda, G., and Wilson, S. K.: Spatial and temporal patterns of mass

582   bleaching of corals in the Anthropocene, Science, 359, 80-83, 2018.

583   Inoue, H. Y., Ishii, M., Matsueda, H., Saito, S., Aoyama, M., Tokieda, T., Midorikawa, T.,

584   Nemoto, K., Kawano, T., Asanuma, I., Ando, K., Yano, T., and Murata, A.: Distributions

585   and variations in the partial pressure of CO_2 in surface waters (pCO$_2$w) of the central

586   and western equatorial Pacific during the 1997/1998 El Niño event, Marine Chemistry,

587   76, 59-75, 2001.

588   IPCC: Climate Change 2007: Synthesis Report. Contribution of Working Groups I, II and III

589   to the Fourth Assessment Report of the Intergovernmental Panel on Climate Change,

590   IPCC, Geneva, Switzerland., 2007. p. 104, 2007.

591   Ishii, M., Inoue, H. Y., Midorikawa, T., Saito, S., Tokieda, T., Sasano, D., Nakadate, A.,

592   Nemoto, K., Metzl, N., Wong, C. S., and Feely, R. A.: Spatial variability and decadal

593   trend of the oceanic CO_2 in the western equatorial Pacific warm/fresh water, Deep Sea

594   Research Part II: Topical Studies in Oceanography, 56, 591-606, 2009.

595   Kelmo, F., Bell, J. J., Moraes, S. S., Gomes, R. d. C. T., Mariano-Neto, E., and Attrill, M. J.:

596   Differential Responses of Emergent Intertidal Coral Reef Fauna to a Large-Scale El-

597   Niño Southern Oscillation Event: Sponge and Coral Resilience, PLOS ONE, 9,

598   e93209, 2014.

599   Klochko, K., Kaufman, A. J., Yao, W., Byrne, R. H., and Tossell, J. A.: Experimental

600   measurement of boron isotope fractionation in seawater, Earth and Planetary Science

601   Letters, 248, 276-285, 2006.

602   Kubota, K., Yokoyama, Y., Ishikawa, T., Suzuki, A., and Ishii, M.: Rapid decline in pH of

603   coral calcification fluid due to incorporation of anthropogenic CO2, Scientific reports, 7,

604   7694, 2017.

605   Kwiatkowski, L., Cox, P., Halloran, P. R., Mumby, P. J., and Wiltshire, A. J.: Coral bleaching

606   under unconventional scenarios of climate warming and ocean acidification, Nature

607   Climate Change, 5, 777, 2015.

608   Langdon, C. and Atkinson, M. J.: Effect of elevated pCO2 on photosynthesis and

609   calcification of corals and interactions with seasonal change in temperature/irradiance

610   and nutrient enrichment, Journal of Geophysical Research: Oceans, 110, C09S07,

611   2005.

612   Lee, K., Kim, T.-W., Byrne, R. H., Millero, F. J., Feely, R. A., and Liu, Y.-M.: The universal
613   ratio of boron to chlorinity for the North Pacific and North Atlantic oceans, Geochimica
614   et Cosmochimica Acta, 74, 1801-1811, 2010.

615   Liu, Y., Peng, Z., Zhou, R., Song, S., Liu, W., You, C. F., Lin, Y. P., Yu, K., Wu, C. C., Wei,
616   G., Xie, L., Burr, G. S., and Shen, C. C.: Acceleration of modern acidification in the
617   South China Sea driven by anthropogenic CO_2, Sci Rep, 4, 5148, 2014.

618   Martínez-Botí, M. A., Marino, G., Foster, G. L., Ziveri, P., Henehan, M. J., Rae, J. W. B.,
619   Mortyn, P. G., and Vance, D.: Boron isotope evidence for oceanic carbon dioxide
620   leakage during the last deglaciation, Nature, 518, 219, 2015.

621   McConnaughey, T. A. and Whelan, J. F.: Calcification generates protons for nutrient and
622   bicarbonate uptake, Earth-Science Reviews, 42, 95-117, 1997.

623   McCulloch, M., Falter, J., Trotter, J., and Montagna, P.: Coral resilience to ocean
624   acidification and global warming through pH up-regulation, Nature Climate Change, 2,
625   623, 2012.

626   McCulloch, M. T., D'Olivo, J. P., Falter, J., Holcomb, M., and Trotter, J. A.: Coral calcification
627   in a changing World and the interactive dynamics of pH and DIC upregulation, Nature
628   Communications, 8, 15686, 2017.

629   Meglen, R. R.: Examining large databases: a chemometric approach using principal
630   component analysis, Marine Chemistry, 39, 217-237, 1992.

631   Millero, F. J.: Chemical Oceanography, Boca Raton, FL: CRC, 2006.

632   Orr, J. C., Fabry, V. J., Aumont, O., Bopp, L., Doney, S. C., Feely, R. A., Gnanadesikan, A.,
633   Gruber, N., Ishida, A., Joos, F., Key, R. M., Lindsay, K., Maier-Reimer, E., Matear, R.,
634   Monfray, P., Mouchet, A., Najjar, R. G., Plattner, G. K., Rodgers, K. B., Sabine, C. L.,
635   Sarmiento, J. L., Schlitzer, R., Slater, R. D., Totterdell, I. J., Weirig, M. F., Yamanaka,
636   Y., and Yool, A.: Anthropogenic ocean acidification over the twenty-first century and its
637   impact on calcifying organisms, Nature, 437, 681-686, 2005.

638   Orr, J. C., Maier-Reimer, E., Mikolajewicz, U., Monfray, P., Sarmiento, J. L., Toggweiler, J.

639   R., Taylor, N. K., Palmer, J., Gruber, N., Sabine, C. L., Le Quéré, C., Key, R. M., and

640   Boutin, J.: Estimates of anthropogenic carbon uptake from four three-dimensional

641   global ocean models, Global Biogeochemical Cycles, 15, 43-60, 2001.

642   Pearson, P. N. and Palmer, M. R.: Middle Eocene Seawater pH and Atmospheric Carbon

643   Dioxide Concentrations, Science, 284, 1824-1826, 1999.

644   Pelejero, C., Calvo, E., McCulloch, M. T., Marshall, J. F., Gagan, M. K., Lough, J. M., and

645   Opdyke, B. N.: Preindustrial to Modern Interdecadal Variability in Coral Reef pH,

646   Science, 309, 2204-2207, 2005.

647   Petit et al.: Climate and atmospheric history of the past 420,000 years from the Vostok ice

648   core, Antarctica, Nature, 399, 429–436, 1999.

649   Raven, J., Caldeira, K., Elderfield, H., Hoegh-Guldberg, O., Liss, P., Riebesell, U.,

650   Shepherd, J., Turley, C., and Watson, A.: Ocean acidification due to increasing

651   atmospheric carbon dioxide, The Royal Society Policy Document 12/05, London, UK,

652   2005.

653   Reynaud, S., Hemming, N. G., Juillet-Leclerc, A., and Gattuso, J.-P.: Effect of pCO_2 and

654   temperature on the boron isotopic composition of the zooxanthellate coral Acropora

655   sp, Coral Reefs, 23, 539-546, 2004.

656   Sabine, C. L., Feely, R. A., Gruber, N., Key, R. M., Lee, K., Bullister, J. L., Wanninkhof, R.,

657   Wong, C. S., Wallace, D. W. R., Tilbrook, B., Millero, F. J., Peng, T.-H., Kozyr, A.,

658   Ono, T., and Rios, A. F.: The Oceanic Sink for Anthropogenic CO_2, Science, 305, 367-

659   371, 2004.

660   Sanyal, A., Hemming, N. G., Broecker, W. S., and Hanson, G. N.: Changes in pH in the

661   eastern equatorial Pacific across stage 5–6 boundary based on boron isotopes in

662   foraminifera, Global Biogeochemical Cycles, 11, 125-133, 1997.

663   Sanyal, A., Hemming, N. G., Hanson, G. N., and Broecker, W. S.: Evidence for a higher pH

664   in the glacial ocean from boron isotopes in foraminifera, Nature, 373, 234-236, 1995.

665   Schulz, M. and Mudelsee, M.: REDFIT: estimating red-noise spectra directly from unevenly

666   spaced paleoclimatic time series, Computers & Geosciences, 28, 421-426, 2002.

667   Shinjo, R., Asami, R., Huang, K.-F., You, C.-F., and Iryu, Y.: Ocean acidification trend in the

668   tropical North Pacific since the mid-20th century reconstructed from a coral archive,

669   Marine Geology, 342, 58-64, 2013.

670   Sutton, A. J., Feely, R. A., Sabine, C. L., McPhaden, M. J., Takahashi, T., Chavez, F. P.,

671   Friederich, G. E., and Mathis, J. T.: Natural variability and anthropogenic change in

672   equatorial Pacific surface ocean pCO_2 and pH, Global Biogeochemical Cycles, 28,

673   131-145, 2014.

674   Takahashi, T., Sutherland, S. C., Chipman, D. W., Goddard, J. G., Ho, C., Newberger, T.,

675   Sweeney, C., and Munro, D. R.: Climatological distributions of pH, pCO_2, total CO_2,

676   alkalinity, and $CaCO_3$ saturation in the global surface ocean, and temporal changes at

677   selected locations, Marine Chemistry, 164, 95-125, 2014.

678   Takahashi, T., Sutherland, S. C., Feely, R. A., and Cosca, C. E.: Decadal Variation of the

679   Surface Water PCO_2 in the Western and Central Equatorial Pacific, Science, 302, 852-

680   856, 2003.

681   Torrence, C. and Compo, G. P.: A practical guide to wavelet analysis. Bulletin of the

682   American Meteorological Society, 79, 61-78, 1998.

683   Trotter, J., Montagna, P., McCulloch, M., Silenzi, S., Reynaud, S., Mortimer, G., Martin, S.,

684   Ferrier-Pagès, C., Gattuso, J.-P., and Rodolfo-Metalpa, R.: Quantifying the pH 'vital

685   effect' in the temperate zooxanthellate coral Cladocora caespitosa: Validation of the

686   boron seawater pH proxy, Earth and Planetary Science Letters, 303, 163-173, 2011.

687   Van Heuven, Pierrot, S., D. , Rae, J. W. B., Lewis, E., and Wallace, D. W. R.: MATLAB

688   Program Developed for CO_2 System Calculations. ORNL/CDIAC-105b. Carbon

689   Dioxide Information Analysis Center, Oak Ridge National Laboratory, U.S. Department

690   of Energy, Oak Ridge, Tennessee, doi: 10.3334/CDIAC/otg.CO2SYS_MATLAB_v1.1,

691   2011. 2011.

692   Vengosh, A., Kolodny, Y., Starinsky, A., Chivas, A. R., and McCulloch, M. T.: Coprecipitation

693   and isotopic fractionation of boron in modern biogenic carbonates, Geochimica et

694   Cosmochimica Acta, 55, 2901-2910, 1991.

695   Wagener, T., Lees, M. J., and Wheater, H. S.: Monte-Carlo analysis toolboxuser manual.

696   Tech. Rep., Civil and Environmental EngineeringDepartment, Imperial College of

697   Science Technology and Medicine, 2001. 2001.

698   Wall, M., Fietzke, J., Schmidt, G. M., Fink, A., Hofmann, L. C., de Beer, D., and Fabricius, K.

699   E.: Internal pH regulation facilitates in situ long-term acclimation of massive corals to

700   end-of-century carbon dioxide conditions, Scientific Reports, 6, 30688, 2016.

701   Wei, G., McCulloch, M. T., Mortimer, G., Deng, W., and Xie, L.: Evidence for ocean

702   acidification in the Great Barrier Reef of Australia, Geochimica et Cosmochimica Acta,

703   73, 2332-2346, 2009.

704   Wei, G., Wang, Z., Ke, T., Liu, Y., Deng, W., Chen, X., Xu, J., Zeng, T., and Xie, L.: Decadal

705   variability in seawater pH in the West Pacific: Evidence from coral $\delta^{11}B$ records,

706   Journal of Geophysical Research: Oceans, 120, 7166-7181, 2015.

707   Wu, H. C., Dissard, D., Douville, E., Blamart, D., Bordier, L., Tribollet, A., Le Cornec, F.,

708   Pons-Branchu, E., Dapoigny, A., and Lazareth, C. E.: Surface ocean pH variations

709   since 1689 CE and recent ocean acidification in the tropical South Pacific, Nature

710   Communications, 9, 2543, 2018.

711   Zeebe, R. E. and Wolf-Gladrow, D. A.: CO_2 in Seawater: Equilibrium, Kinetics, Isotopes,

712   Amsterdam: Elsevier, 2001. 2001.

713